16th World Conference on Earthquake Engineering, 16WCEE 2017

Santiago Chile, January 9th to 13th 2017

Paper N° 2772 (Abstract ID)

Registration Code: S-E1464705294

SIMULATION OF STRONG MOTION TIME HISTORY FOR THE 2011 TOHOKU EARTHQUAKE WITH CONSIDERATIONS OF MULTIPLE NONLINEAR EFFECTS

A. Nozu(1)

(1) Director of Earthquake Disaster Prevention Engineering Division, Port and Airport Research Institute, nozu@pari.go.jp

Abstract

To predict strong ground motions for future large earthquakes including huge subduction earthquakes, it is important to take into account the effects of soil nonlinearity. The author has been developing a simple method to simulate strong ground motions taking into account the effects of soil nonlinearity (e.g., Nozu and Morikawa, 2003). One of the key concepts involved in our method is the multiple nonlinear effects. In general, a seismic ray connecting the source and the site usually crosses the soft soil layers several times except for the direct S wave. Therefore, the seismic wave is affected by soil nonlinearity several times during the propagation from the source to the receiver. This phenomenon is referred to as "the multiple nonlinear effects". The simplified method used in this study considers the multiple nonlinear effects. It uses two parameters to represent the effects of soil nonlinearity; one representing the reduction of averaged shear wave velocity within the sediment (ν_1) and the other representing the increase of averaged damping factor within the sediment (ν_2). The method has been applied to the 2000 Western Tottori earthquake, etc. (e.g., Nozu and Morikawa, 2003). The method, however, has been validated only for a limited amount of strong motion data, partly because there was only a limited amount of strong motion data affected by soil nonlinearity. Therefore, in this article, making use of strong motion data for the 2011 Tohoku earthquake and the source model developed for the same earthquake by the author (Nozu, 2012), strong motion simulation with considerations of soil nonlinearity was conducted and its effectiveness was studied. In particular, strong motion records with the evident effects of soil nonlinearity were selected and they were simulated using the source model and taking into account empirical site amplification and phase effects (Nozu et al., 2009). Soil nonlinearity was considered using the method of Nozu and Morikawa (2003). Among the parameters involved in the method, ν_1 was basically determined based on Wakai and Nozu (2013) and ν_2 was determined so that the observed ground motion could be simulated as accurately as possible. As a result, it was found that, the duration of strong ground motions tended to be overestimated if the parameter ν_2 was not used for the sites with the effect of soil nonlinearity. In each of the target sites, by using these two parameters, the simulation result was improved. Thus, the effectiveness of strong motion simulation with considerations of soil nonlinearity was confirmed. Based on the results, the application of the method for future earthquakes was also discussed.

Keywords: The 2011 Tohoku earthquake; Soil nonlinearity; Strong motion simulation; Multiple nonlinear effects

1. Introduction

To predict strong ground motions for future large earthquakes including huge subduction earthquakes, it is important to take into account the effects of soil nonlinearity [1, 2]. The author has been developing a simple method to simulate strong ground motions taking into account the effects of soil nonlinearity [3]. The method considers the multiple nonlinear effects as will be explained later, and it has been applied to the 2000 Western Tottori earthquake, etc. [3]. The method, however, has been validated only for a limited amount of strong motion data, partly because there was only a limited amount of strong motion data affected by soil nonlinearity. Therefore, in this article, making use of strong motion data for the 2011 Tohoku earthquake [4, 5] and the source model developed for the same earthquake by the author [6, 7], strong motion simulation with considerations of soil nonlinearity was conducted and its effectiveness was studied. In particular, strong motion records with the evident effects of soil nonlinearity were selected and they were simulated using the source model and taking into account empirical site amplification and phase effects [8, 9]. Soil nonlinearity was considered using the method of Nozu and Morikawa [3]. The method uses two parameters to represent the effects of soil nonlinearity; one representing the reduction of averaged shear wave velocity within the sediment (ν_1) and the other representing the increase of averaged damping factor within the sediment (ν_2). In the simulation, ν_1 was basically determined based on Wakai and Nozu [10] and ν_2 was determined so that the observed ground motion could be simulated as accurately as possible. Based on the results, the application of the method for future earthquakes was also discussed.

2. Method

One of the key concepts involved in our method [3] is the multiple nonlinear effects (Fig. 1). Conventional approaches for evaluating the effects of soil nonlinearity are often based on the assumption that the seismic wave is affected by soil nonlinearity only after its incidence to the local soft soil layers. If we consider a seismic ray connecting the source and the site, however, it usually crosses the soft soil layers several times as illustrated in Fig. 1 except for the direct S wave. Therefore, it is more reasonable to assume that the seismic wave is affected by soil nonlinearity several times during the propagation from the source to the receiver. In this case the incident wave at the bottom of the local soft soil layers is already affected by soil nonlinearity. This phenomenon is referred to as "the multiple nonlinear effects" [3]. In spite of the potential importance of the multiple nonlinear effects, it has seldom been addressed in the literature probably because soil nonlinearity has mainly been assessed in terms of spectral amplitude or peak acceleration rather than the time history itself. Once time history of strong ground motion is examined, however, evidence of the multiple nonlinear effects can be clearly recognized as described in the later sections of this article, because the multiple nonlinear effects is especially evident in the later portions of the recorded ground motions.

The method used in this study [3] considers the multiple nonlinear effects. One of the key assumptions in the present method is that the delay of an arbitrary later phase found on the Green's function is caused by the trapping of the seismic ray within the sedimentary basin as schematically illustrated in Fig 2. In other words, it is assumed that the site effects, rather than the path effects, are predominant in the phase information of the Green's function. Thus the difference of the arrival times of the direct-S phase and the later phase $t-t_0$ is approximately equal to the time for which the seismic ray corresponding to the later phase is trapped within the sedimentary basin. It is important in this discussion to recognize that the time history in Fig. 2 is a Green's function instead of a main shock ground motion. Because the source time function for a Green's function is impulsive, different arrivals found on the Green's function can be regarded to have started the hypocenter at the same time and, therefore, the difference in the arrival times can be attributed to the difference of the time spent along the ray.

In case of a strong excitation, the materials within the sedimentary basin can exhibit nonlinear behavior including the reduction in shear wave velocity and the increase in damping [2]. The nonlinear behavior is typically most prominent near the surface of the basin as illustrated in Fig. 1. Due to the nonlinear behavior, the arrival time of a later phase will be delayed and the amplitude of the later phase will be reduced. To consider these effects, two parameters, ν_1 and ν_2, are used to represent the deviation of material properties of the sediments from linear status due to soil nonlinearity. The parameter ν_1 is defined as the averaged reduction in

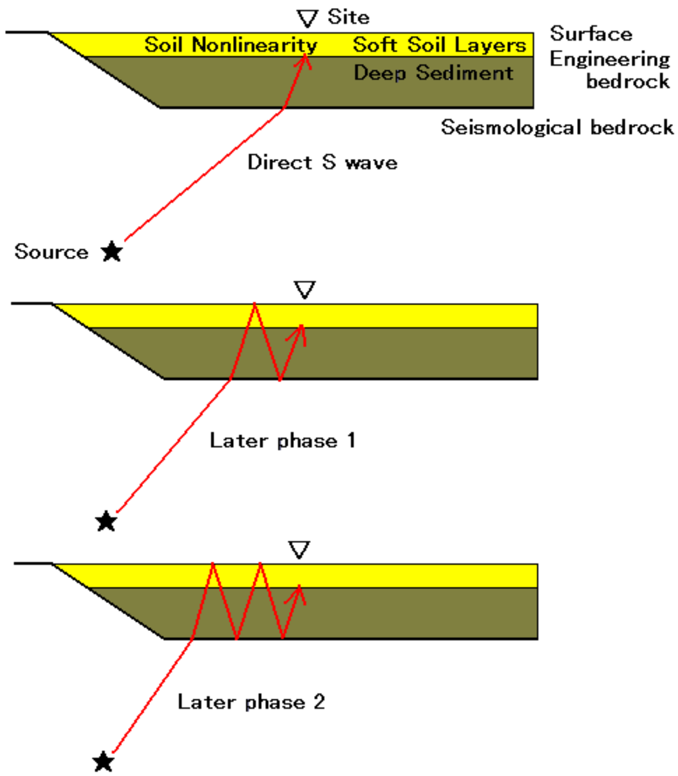

Fig. 1 – The concept of multiple nonlinear effects

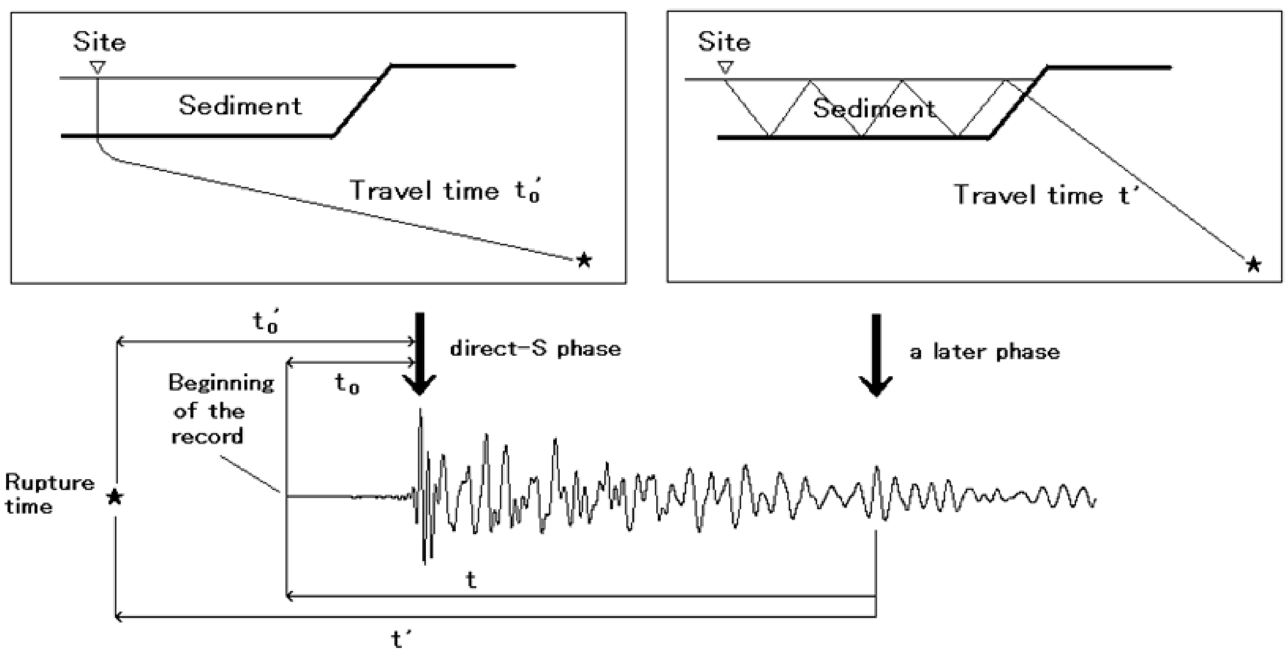

Fig. 2 – Examples of the direct S phase and a later phase involved in a Green's function

shear wave velocity along the ray in the sediments, that is, $\nu_1 = V_s/V_{s0}$, where V_s is the shear wave velocity for a strong motion and V_{s0} is the shear wave velocity for a weak motion. The parameter ν_2 is defined as the averaged increase in damping factor along the ray in the sediments, that is, $\nu_2 = h - h_0$, where h is the damping factor for a strong motion and h_0 is the damping factor for a weak motion. Then, in case of a strong excitation, the seismic ray corresponding to the later phase will be trapped within the sedimentary basin $1/\nu_1$ times longer than the linear case. At the same time, the amplitude of the later phase will be reduced by a factor of $\exp[-\nu_2\ \omega(t-t_0)]$, because $t-t_0$ is approximately equal to the time for which the seismic ray corresponding to the later phase is trapped within the sedimentary basin as discussed above. As a result, the Green's function is modified as follows:

$$g_n(t)=g(t) \qquad \text{for } t<t_0 \text{ and}$$

$$g_n(t_0+(t-t_0)/\nu_1)=g(t) \quad \exp[-\nu_2 \quad \omega(t-t_0)] \qquad \text{for} \quad t>t_0, \tag{1}$$

where $g(t)$ is the original Green's function and $g_n(t)$ is the Green's function after modification. The parameters ν_1 and ν_2 are referred to as "the nonlinear parameters" [3]. Because ω is involved in Equation (1) the Green's function should be, at first, decomposed into components having different frequencies and then each component should be modified based on Equation (1). Finally, the modified components should be summed up.

3. Source model and calculation of strong ground motions

Making use of strong motion data for the 2011 Tohoku earthquake [4, 5] and the source model developed for the same earthquake by the author [6, 7], strong motion simulation with considerations of soil nonlinearity was conducted and its effectiveness was studied. In particular, strong motion records with the evident effects of soil nonlinearity were selected and they were simulated using the source model and taking into account empirical site amplification and phase effects [8, 9].

Fig. 3 shows the source model used for the study [6, 7]. The source model involves 9 SPGAs (Strong-motion Pulse Generation Areas), located off the coast of Miyagi through Ibaraki. The model can basically explain the time history of the observed strong ground motions at stiff sites along the coast of Miyagi through Ibaraki, especially in the frequency range relevant to structural damage, with linear calculations [6, 7].

Fig. 3 and Table 1 show the stations used for this study. These stations were selected because the effect of soil nonlinearity was evident at these stations.

Strong ground motions were calculated based on site amplification and phase characteristics [8, 9], to take into account the effect of sediments for both the Fourier amplitude and phase of strong ground motions. An outline of the method follows. The first step is to evaluate ground motions from a small event (Green’s function). The Fourier amplitude of the Green's function is evaluated as a product of the source spectrum $|S(f)|$, the path effect $|P(f)|$ and the site amplification factor $|G(f)|$. The source spectrum was assumed to follow the ω^{-2} model [11]. Geometrical spreading and non-elastic attenuation were considered for the path effect [12]. The empirical site amplification factors [13] were used. The Fourier phase of an actual record of a small earthquake at the site of interest was used for the Fourier phase of the Green's function. Thus, we obtained a time domain Green's function which incorporates the effects of sediments both on the Fourier amplitude and Fourier phase. The Green’s function in the frequency domain can be written as follows:

$$|S(f)|\ |P(f)|\ |G(f)|\ O_s(f)\ /\ |O_s(f)|_p, \tag{2}$$

where $O_s(f)$ is the Fourier transform of an actual record at the site of interest and $|Os(f)|_p$ is its Parzen-windowed amplitude (a band width of 0.05 Hz was used). If several records are available for the site, it is preferable to choose an event that has a similar incident angle and a similar back-azimuth to the target event. The second step is to superpose Green's functions to obtain strong ground motions from a large event (or a subevent of a large event) in the same way as the EGF method [14, 15]. When soil nonlinearity is considered, the time domain Green’s function is corrected with the method described previously.

For the particular application to the Tohoku earthquake, the averaged radiation coefficient of 0.63 was used. The parameter *PRTITN* [12], which represents the partition of S-wave energy into two horizontal components, was determined to be compatible with the observed records. For the S-wave velocity and the density in the source region, 3.9 km/s and 3.1×10^3 kg/m^3 were used [16, 17]. For the path effect, the Q value estimated for the region was used ($Q=114\ f^{\,0.92}$) [18].

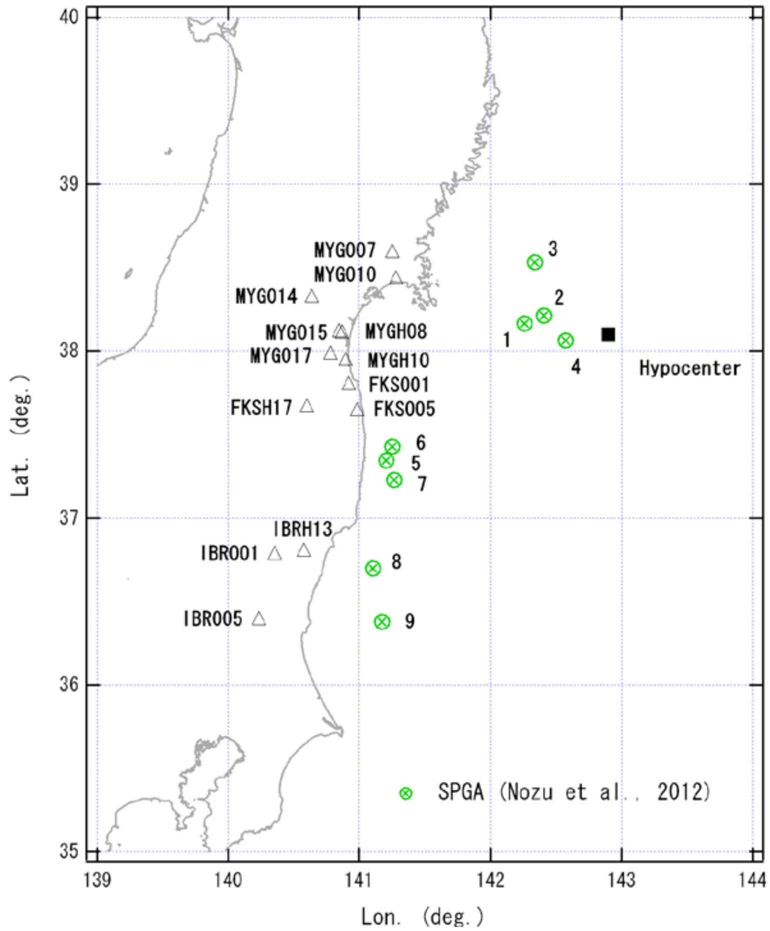

Fig. 3 – Target sites and the source model [6, 7]

Table 1 – The target sites and the nonlinear parameters manually determied for each site

Site	ν1	ν2	Comments
MYG007	0.68	0.002	
MYG010	0.71	0.020	
MYG014	0.78	0.003	
MYG015	0.67	0.011	In Nozu(2012), ν2=0.010
MYG017	0.66	0.015	
MYGH08	0.82	0.006	
MYGH10	0.47*	0.006	In Nozu(2012), ν2=0.008
FKS001	0.90	0.005	In Nozu(2012), ν2=0.005
FKS005	0.90	0.006	In Nozu(2012), ν2=0.005
FKSH17	0.84	0.002	
IBR001	0.78	0.006	
IBR005	0.78	0.018	
IBRH13	0.78	0.005	

* For MYGH10, ν_1=0.80 was used for the former part of the waveforms for which SPGA1-3 contribute and ν_1=0.47 was used for the later part of the waveforms for which SPGA4-9 contribute.

Table 2 – Small events used for the analysis

	SPGA1	SPGA2	SPGA3	SPGA4	SPGA5	SPGA6	SPGA7	SPGA8	SPGA9
MYG007	20051217		20021103	20051217					
MYG010	20050816		20021103	20131101					
MYG014	20051217		20021103	20051217					
MYG015	20051217	Same as left	20021103	20131101	Same as left	Same as left	Same as left	Same as left	Same as left
MYG017	20051217		20021103	20051217					
MYGH08	20050816		20021103	20090801					
MYGH10	20050816		20021103	20110309					
FKS001	20050816		20021103	20090801					
FKS005	20050816	Same as left	Same as left	20090801	20051022	Same as left	Same as left	20091023	20080508
FKSH17	20051217				20051022			20091023	20080508
IBR001	20051217	Same as left	Same as left	Same as left	20051022	Same as left	Same as left	20091023	20080508
IBR005	20051217				20051022			20091023	20080508
IBRH13	20051218				20051023			20091023	20080508

The small events listed in Table 2 were used to determine the Fourier phase of the Green's functions. These events were selected taking into account the similarity of the incident angle and the back-azimuth between the small events and the SPGAs.

4. Results for manually determined nonlinear parameters

In the simulation, the nonlinear parameters were manually determined with the aim of reproducing the observed ground motions as accurately as possible as shown in Table 1. Among the nonlinear parameters, ν_1 was basically determined by referring to the ratio of the peak frequencies of strong and weak motions at the same site [10], because the parameter ν_1 represents the ratio of the shear wave velocities within the sediments between the linear and nonlinear cases, and thus ν_1 represents the ratio of the resonant frequencies of the sediments between the linear and nonlinear cases. Then, the parameter ν_2 was determined so that the observed ground motion could be simulated as accurately as possible, with special reference to the duration of the later phases.

Fig. 4 compares the observed and synthetic Fourier spectra at MYG010. The synthetic spectrum in the left panel corresponds to the linear calculation. In this case, the peak frequency of the synthetic spectrum is around 1.0 Hz and it is not consistent with the observed peak frequency. This discrepancy was caused by the nonlinear soil behavior. Then, at first, the parameter ν_1 was introduced to consider the reduction of shear wave velocity. The middle panel of Fig. 4 shows the result for this case. The synthetic peak frequency approached to the observed one. However, the amplitude was significantly overestimated. Fig. 5 compares the observed and synthetic velocity waveforms for this case. The amplitude of the later phase was significantly overestimated. Then, finally, the parameter ν_2 was introduced to consider the increase in damping factor. The right panel of Fig. 4 shows the comparison of the Fourier spectra for this case. Fig. 6 shows the comparison of the velocity waveforms for this case. It can be recognized that the result was significantly improved by introducing these parameters. Figs. 7-9 show the same results for another station MYG015. The same tendency can be found.

Fig. 10 shows the relations between the observed and synthetic PSI values at all the stations. Again, the synthetic values approached to the observed ones when both ν_1 and ν_2 were introduced. The PSI value is defined as the square root of the integration of the squared velocity waveforms and it correlates well with the damage to port structures.

5. Iteration scheme

In the above simulation, the nonlinear parameters were manually determined with the aim of reproducing the observed ground motions as accurately as possible, that is, the parameters were optimized for each station.

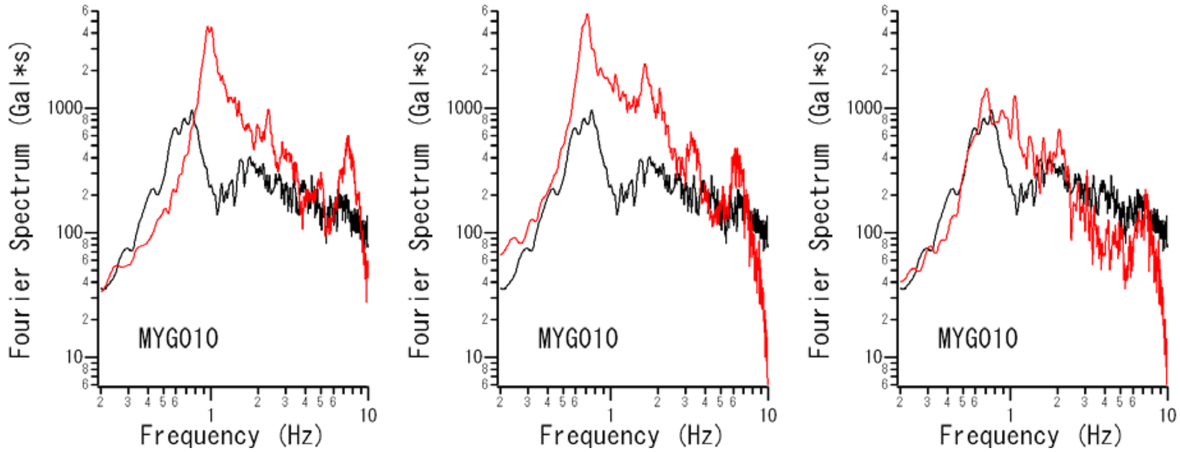

Fig. 4 – Observed (black) and synthetic (red) Fourier spectra at MYG010. The synthetic spectrum was obtained with a linear calculation (left), with only ν_1 (center), and with both ν_1 and ν_2 (right).

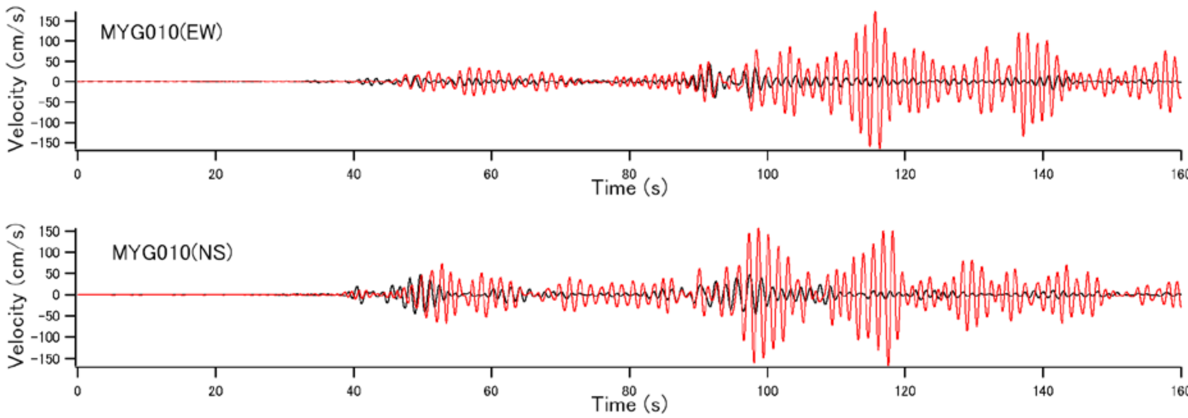

Fig. 5 – Observed (black) and synthetic (red) velocity waveforms at MYG010 (0.2-1 Hz). The synthetic waveforms were obtained with only ν_1.

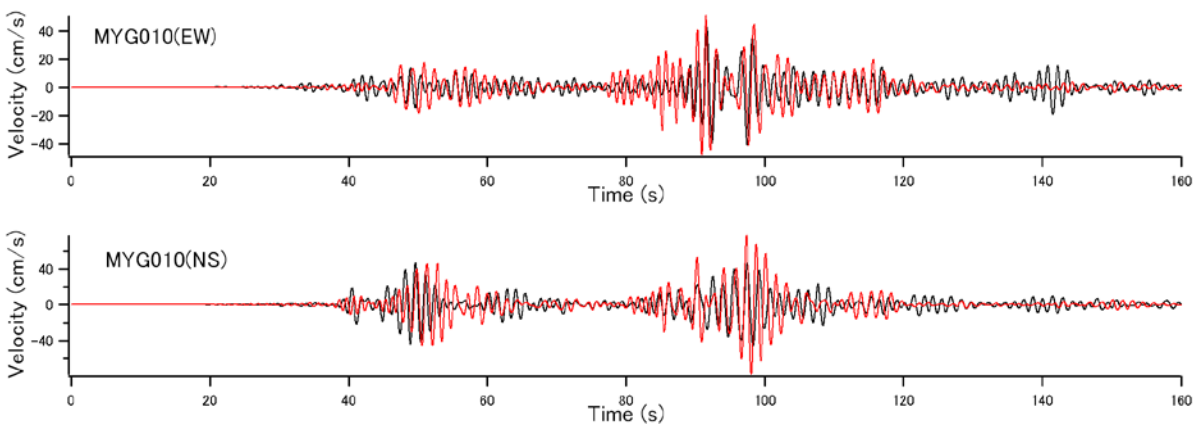

Fig. 6 – Observed (black) and synthetic (red) velocity waveforms at MYG010 (0.2-1 Hz). The synthetic waveforms were obtained with both ν_1 and ν_2.

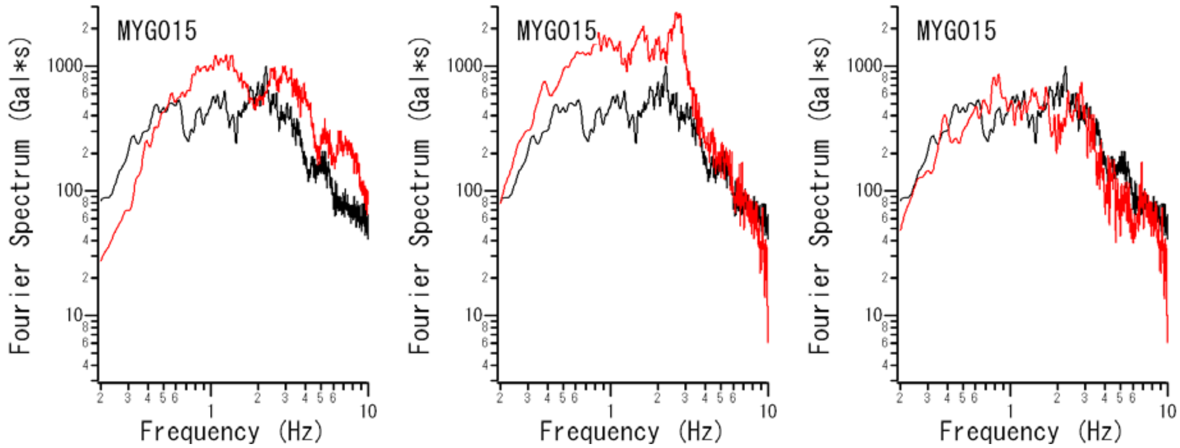

Fig. 7 – Observed (black) and synthetic (red) Fourier spectra at MYG015. The synthetic spectrum was obtained with a linear calculation (left), with only ν_1 (center), and with both ν_1 and ν_2 (right).

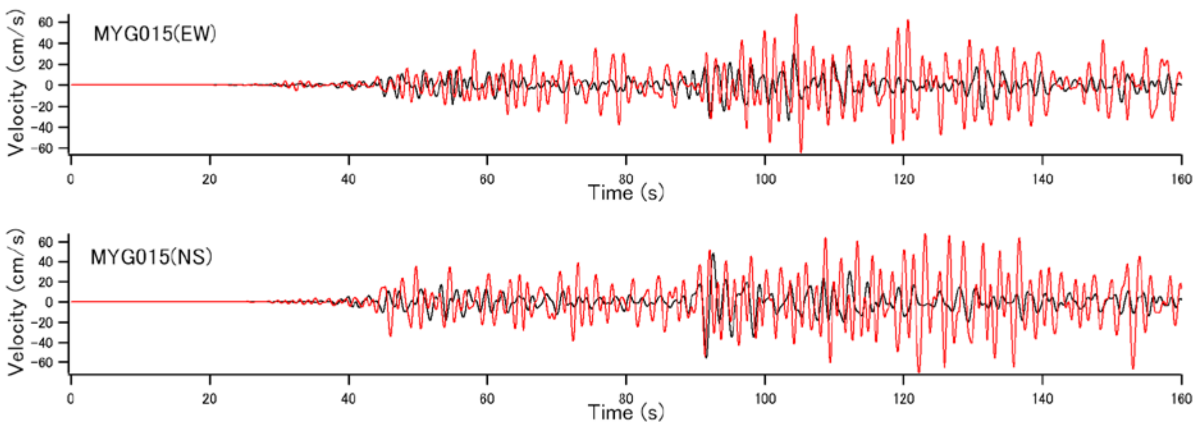

Fig. 8 – Observed (black) and synthetic (red) velocity waveforms at MYG015 (0.2-1 Hz). The synthetic waveforms were obtained with only ν_1.

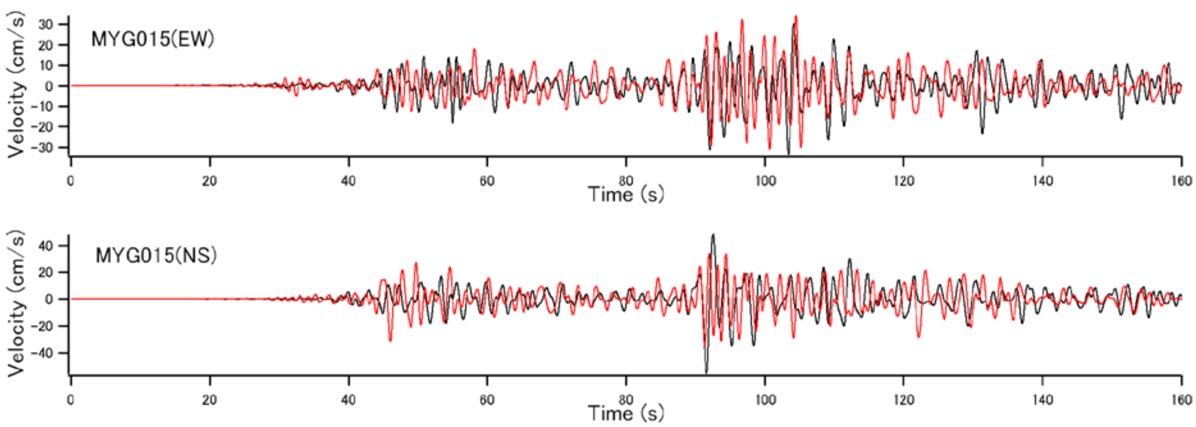

Fig. 9 – Observed (black) and synthetic (red) velocity waveforms at MYG015 (0.2-1 Hz). The synthetic waveforms were obtained with both ν_1 and ν_2.

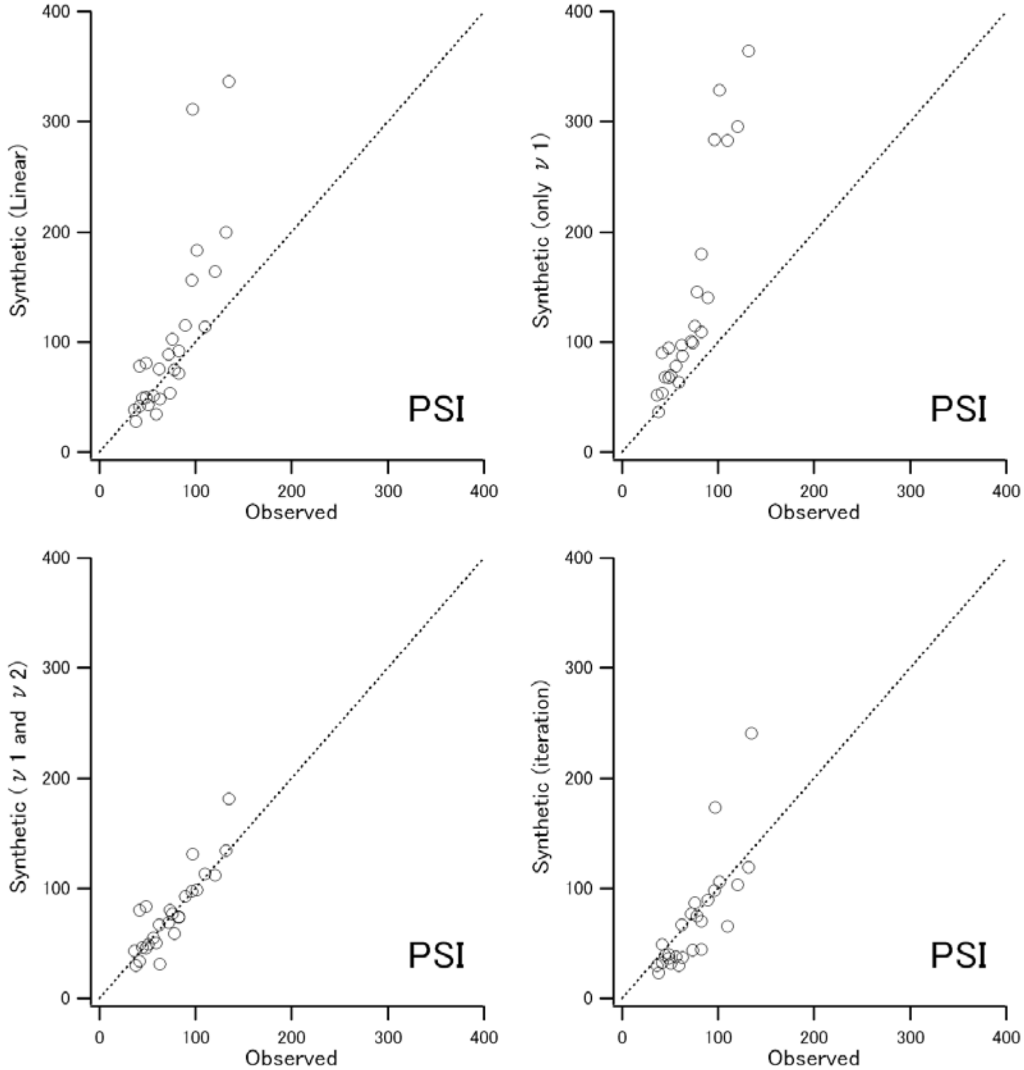

Fig. 10 – Relations between the observed and synthetic PSI values at all the stations. The synthetic values were obtained with a linear calculation (top left), with only ν_1 (top right), and with both ν_1 and ν_2 (bottom left). In the bottom right panel, the synthetic values were obtained with ν_1 and ν_2 determined through the iteration scheme.

However, to apply the same method to the prediction problems, it is not possible to determine the parameters by referring to the observed records, of cause. Thus, the author proposed an iteration scheme to determine the nonlinear parameters, referring to the “equivalent linear analysis” [19], that has been used for a long time in the field of geotechnical earthquake engineering.

In the proposed iteration scheme, the parameter ν_1 is determined from the peak ground velocity (PGV) (cm/s) as follows.

$$\nu_1 = 1/(1+0.0082\ \mathrm{PGV}) \tag{3}$$

Equation (3) is an empirical equation proposed by Wakai and Nozu [10], referring to the observed records during the 2011 Tohoku earthquake. On the other hand, the parameter ν_2 is determined based on the mean curve shown in Fig. 11, which summarizes the result of the analysis described above. The mean curve can be written as

$$\nu_2 = 0.020\ (1 - \nu_1^2), \tag{4}$$

where the functional form was determined referring to Hardin and Drenevich [20].

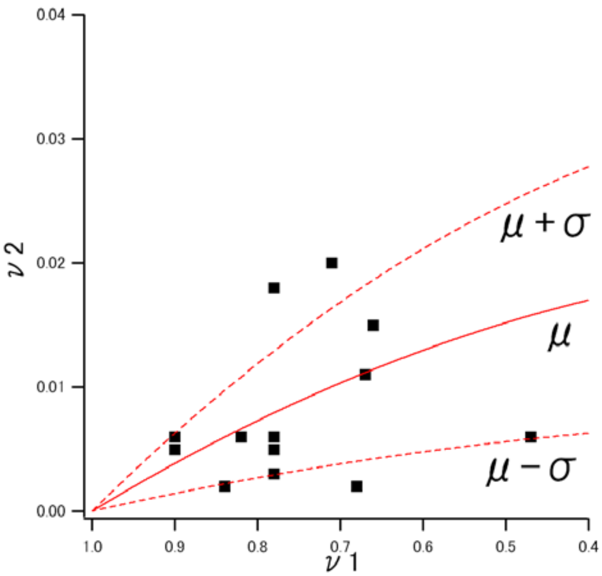

Fig. 11 – Relations between the manually-determined nonlinear parameters ν_1 and ν_2

Fig. 12 compares the observed and synthetic velocity waveforms at MYG010, MYG015, FKS001 and FKSH17, where the synthetic ones were obtained with the nonlinear parameters ν_1 and ν_2 determined through the proposed iteration scheme. It can be observed that the main features of the observed waveforms can be reproduced with the iteration scheme. Finally the bottom right panel of Fig. 10 shows the relations between the observed and synthetic PSI values at all the stations, where the synthetic values were obtained with ν_1 and ν_2 determined through the proposed iteration scheme. It can be observed that, by using the iteration scheme, the PSI values approach to the observed ones, compared to the linear cases.

6. Concluding remarks

To predict strong ground motions for future large earthquakes including huge subduction earthquakes, it is important to take into account the effects of soil nonlinearity [1, 2]. The author has been developing a simple method to simulate strong ground motions taking into account the effects of soil nonlinearity [3]. The method considers the multiple nonlinear effects as will be explained later, and it has been applied to the 2000 Western Tottori earthquake, etc. [3]. The method, however, has been validated only for a limited amount of strong motion data, partly because there was only a limited amount of strong motion data affected by soil nonlinearity. Therefore, in this article, making use of strong motion data for the 2011 Tohoku earthquake [4, 5] and the source model developed for the same earthquake by the author [6, 7], strong motion simulation with considerations of soil nonlinearity was conducted and its effectiveness was studied. In particular, strong motion records with the evident effects of soil nonlinearity were selected and they were simulated using the source model and taking into account empirical site amplification and phase effects [8, 9]. Soil nonlinearity was considered using the method of Nozu and Morikawa [3]. The method uses two parameters to represent the effects of soil nonlinearity; one representing the reduction of averaged shear wave velocity within the sediment ($\nu 1$) and the other representing the increase of averaged damping factor within the sediment ($\nu 2$). In the simulation, $\nu 1$ was basically determined based on Wakai and Nozu [10] and $\nu 2$ was determined so that the observed ground motion could be simulated as accurately as possible. As a result, it was found that, the duration of strong ground motions tended to be overestimated if the parameter $\nu 2$ was not used for the sites with the effect of soil nonlinearity. In each of the target sites, by using these two parameters, the simulation result was improved. Thus, the effectiveness of strong motion simulation with considerations of soil nonlinearity was confirmed. Based on the results, the application of the method for future earthquakes was also discussed.

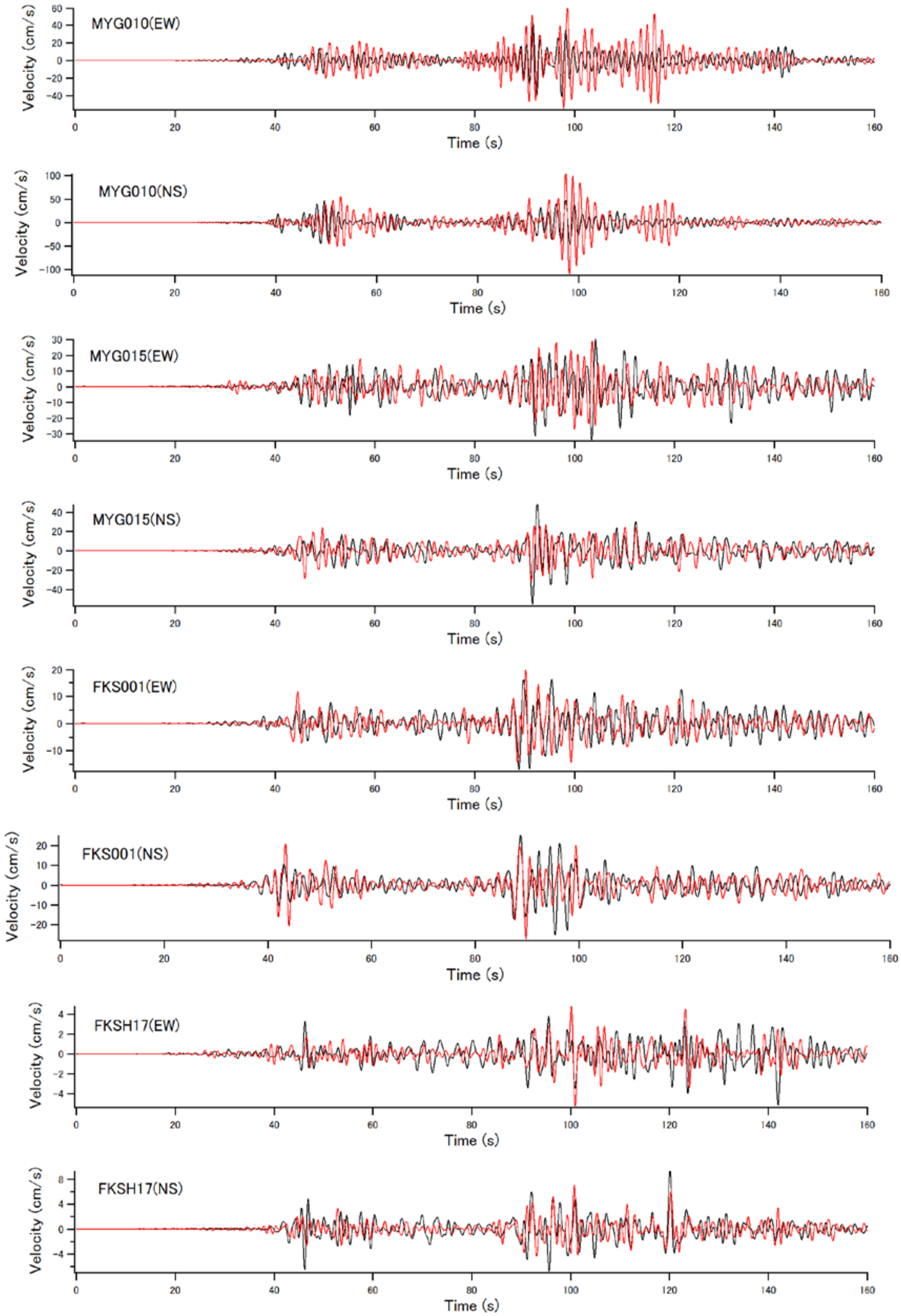

Fig. 12 – Observed (black) and synthetic (red) velocity waveforms at MYG010, MYG015, FKS001 and FKSH17 (0.2-1 Hz). The synthetic ones were obtained with the nonlinear parameters ν_1 and ν_2 determined through the iteration scheme.

7. Acknowledgements

The author would like to thank the National Research Institute for Earth Science and Disaster Prevention (NIED) for providing important strong motion data.

8. References

[1] Aki K (1993): Local site effects on weak and strong ground motion, *Tectonophysics*, **218**, 93-111.

[2] Beresnev IA, Wen KL (1996): Nonlinear soil response: a reality?, *Bull. Seism. Soc. Am.*, **86**, 1964-1978.

[3] Nozu A, Morikawa H (2003): An empirical Green's function method considering multiple nonlinear effects, *Zisin*, **55**, 361-374.

[4] Kinoshita S (1998): Kyoshin Net (K-net), *Seism. Res. Lett*, **69**, 309-332.

[5] Aoi S, Obara K, Hori S, Kasahara K, Okada Y (2000): New strong-motion observation network: KiK-net, *Eos*, Trans. Am. Geophys. Union, **81**, 329.

[6] Nozu A (2014): A super asperity model for the 2011 off the Pacific coast of Tohoku earthquake, *Journal of Japan Association for Earthquake Engineering*, **14**(6), 36-55.

[7] Nozu A, Yamada M, Nagao T, Irikura K (2014): Generation of strong motion pulses during huge subduction earthquakes and scaling of their generation areas, *Journal of Japan Association for Earthquake Engineering*, **14**(6), 96-117.

[8] Nozu A, Nagao T, Yamada M (2006): Simulation of strong ground motions based on site-specific amplification and phase characteristics. *Third Int. Symp. Effects of Surface Geol. on Seism. Motion*, Grenoble, France.

[9] Nozu A, Nagao T, Yamada M (2009): Simulation of strong ground motions using empirical site amplification and phase characteristics – modification to incorporate causality –, *Journal of JSCE*, Ser. A, **65**, 808-813 (in Japanese with English abstract).

[10] Wakai A, Nozu A (2013): General tendency of nonlinear behavior of soft soil deposits during the 2011 off the Pacific coast of Tohoku earthquake, *Tec. Note of Port and Airport Res. Inst.*, No.1272 (in Japanese with English abstract).

[11] Aki K (1967): Scaling law of seismic spectrum, *J. Geophys. Res*, **71**, 1217-1231.

[12] Boore DM (1983): Stochastic simulation of high-frequency ground motions based on seismological models of the radiated spectra, *Bull. Seism. Soc. Am.*, **73**, 1865-1894.

[13] Nozu A, Nagao T (2005): Site amplification factors for strong-motion sites in Japan based on spectral inversion technique, *Tec. Note of Port and Airport Res. Inst.*, No.1102 (in Japanese with English abstract).

[14] Irikura K, Kagawa T, Sekiguchi H (1997): Revision of the empirical Green's function method by Irikura (1986), *SSJ Fall Meeting*, B25 (in Japanese).

[15] Miyake H, Iwata T, Irikura K (2003): Source characterization for broadband ground-motion simulation: kinematic heterogeneous source model and strong motion generation area, *Bull. Seism. Soc. Am.*, **93**, 2531-2545.

[16] Headquaters for Earthquake Research Promotion (2002): Method to evaluate strong ground motions for the anticipated off Miyagi Prefecture earthquake, http://www.jishin.go.jp/main/kyoshindo/02oct_miyagi1/index.htm.

[17] Headquaters for Earthquake Research Promotion (2005): Evaluation of strong ground motions for the anticipated off Miyagi Prefecture earthquake (corrected version), http://www.jishin.go.jp/main/kyoshindo/05dec_miyagi/index.htm.

[18] Satoh T, Tatsumi Y (2002): Source, path and site effects for crustal and subduction earthquakes inferred from strong motions records in Japan, *J. Struct. Constr. Eng.*, AIJ, No.556, 15-24 (in Japanese with English abstract).

[19] Schnabel PB, Lysmer J, Seed HB (1972): SHAKE - A computer program for earthquake response analysis of horizontally layered sites, Report No. EERC 72-12, Col. of Eng., University of California at Berkeley.

[20] Hardin BO, Drenevich VP (1972): Shear modulus and danping in soils: design equations and curves, *Proc. of the American Society of Civil Engineers*, **98**(SM7), 667-692.